WEBINAR SERIES ON ADVANCED AIR MOBILITY

Acknowledgement

The presenter wishes to acknowledge the IEEE Vehicular Technology Society for their sponsorship of the Webinar Series on Advanced Air Mobility.

WEBINAR SERIES ON ADVANCED AIR MOBILITY

Joint Sensing and Communications

K.V.S. Hari

Professor, Department of ECE

Indian Institute of Science, Bangalore

hari@iisc.ac.in, k.hari@ieee.org

1 May 2023

Recap

UAS-to-UAS Communications

In September 2022, The Radio Technical Commission for Aeronautics (RTCA) identified five use cases for UAS to UAS communications.

1. Collision Avoidance
2. Merging/spacing and sequencing of Traffic
3. Airborne Separation
4. Airborne Rerouting
5. Sensing and Sharing of Airspace Hazard Information

IEEE P1920.2 WG is developing a standard for UAS-to-UAS Communications which is expected to be released by the end of 2023.

Key Concepts in Airspace Management

- Air Corridors: Structured airspaces reserved (to some extent) for AAM services
- Geofences: virtual three dimensional “boundaries” each UAS flies within
- UAS-to-UAS Communications: An alternative solution for traffic coordination

Challenge: Detect And Avoid

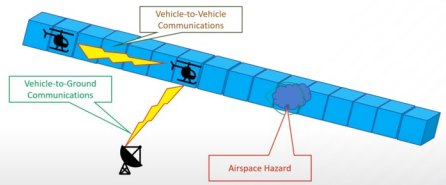

Ref: Webinar by Prof Kamesh Namuduri

Recap

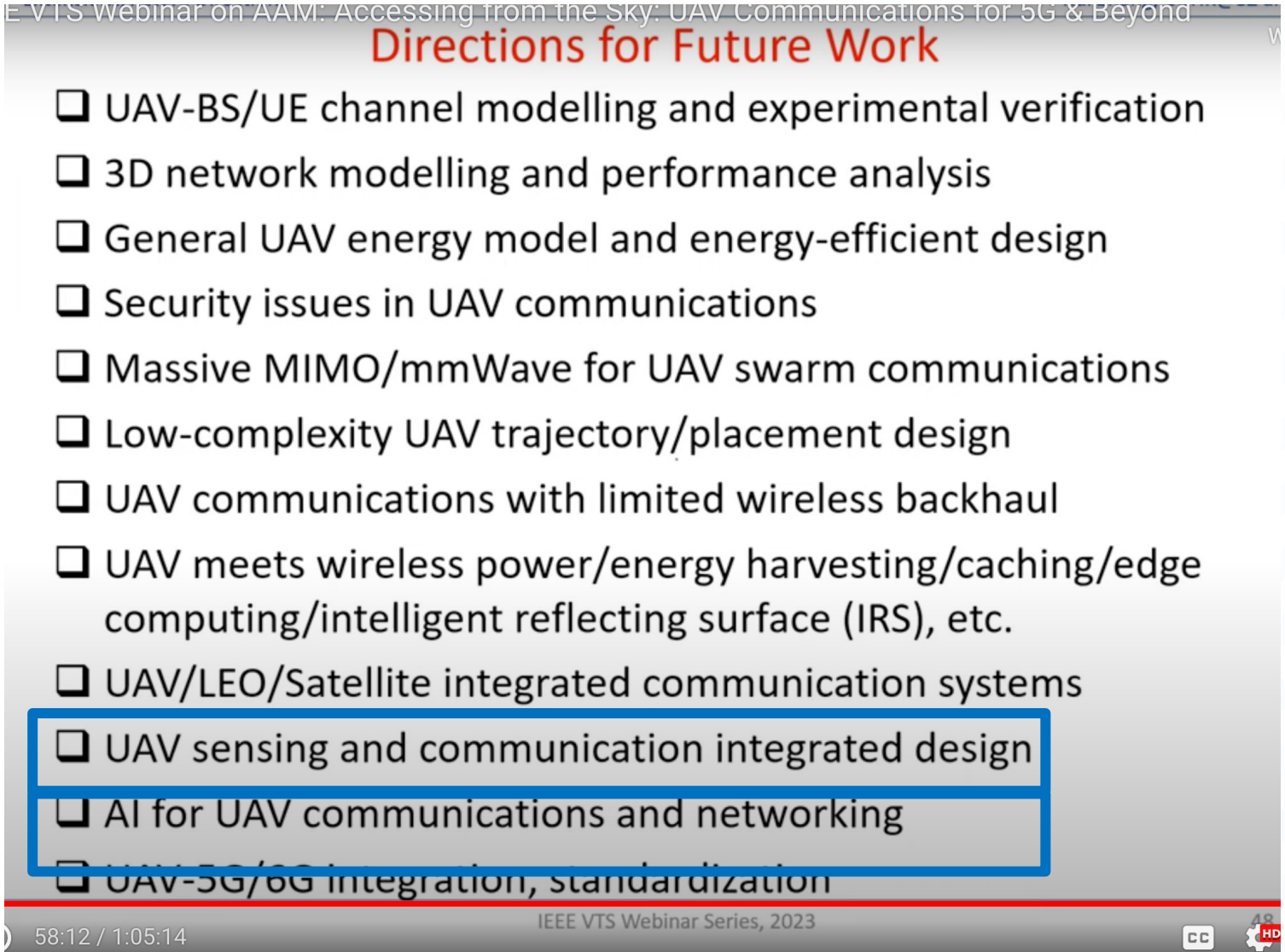

Ref: Webinar by Prof Rui Zhang

Beyond 5G and towards 6G

NEXT-GENERATION wireless networks demand high-quality wireless connectivity as well as highly accurate and robust sensing capability.

Sensing will play a more significant role than ever before.

The close cooperation of the communication and sensing functions can enable significant improvement of **spectrum efficiency, reduction of device size, cost and power consumption and improvement of performance** of both functions.

Space-Air-Ground Integrated Networks

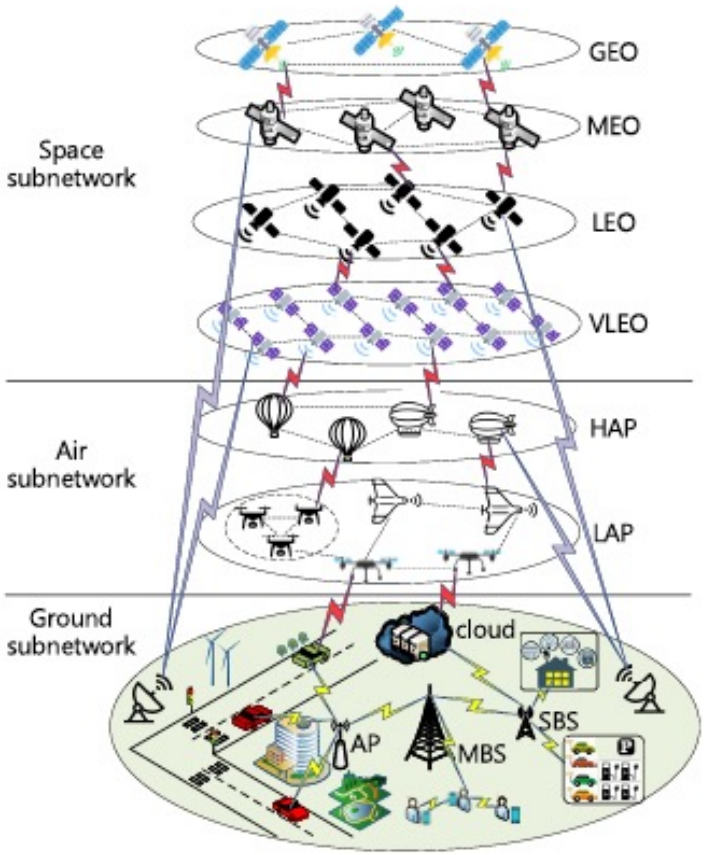

Fig. 2. Architecture of SAG-IoT.

Y. Wang, Z. Su, J. Ni, N. Zhang and X. Shen, "Blockchain-Empowered Space-Air-Ground Integrated Networks: Opportunities, Challenges, and Solutions," in *IEEE Communications Surveys & Tutorials*, vol. 24, no. 1, pp. 160-209, 2022, doi: 10.1109/COMST.2021.3131711.

Joint (Integrated) Sensing and Communication Scenario

Sensing collects and extracts information from noisy observations.

Communication focuses on transferring information via specifically tailored signals and then recovering it from a noisy environment.

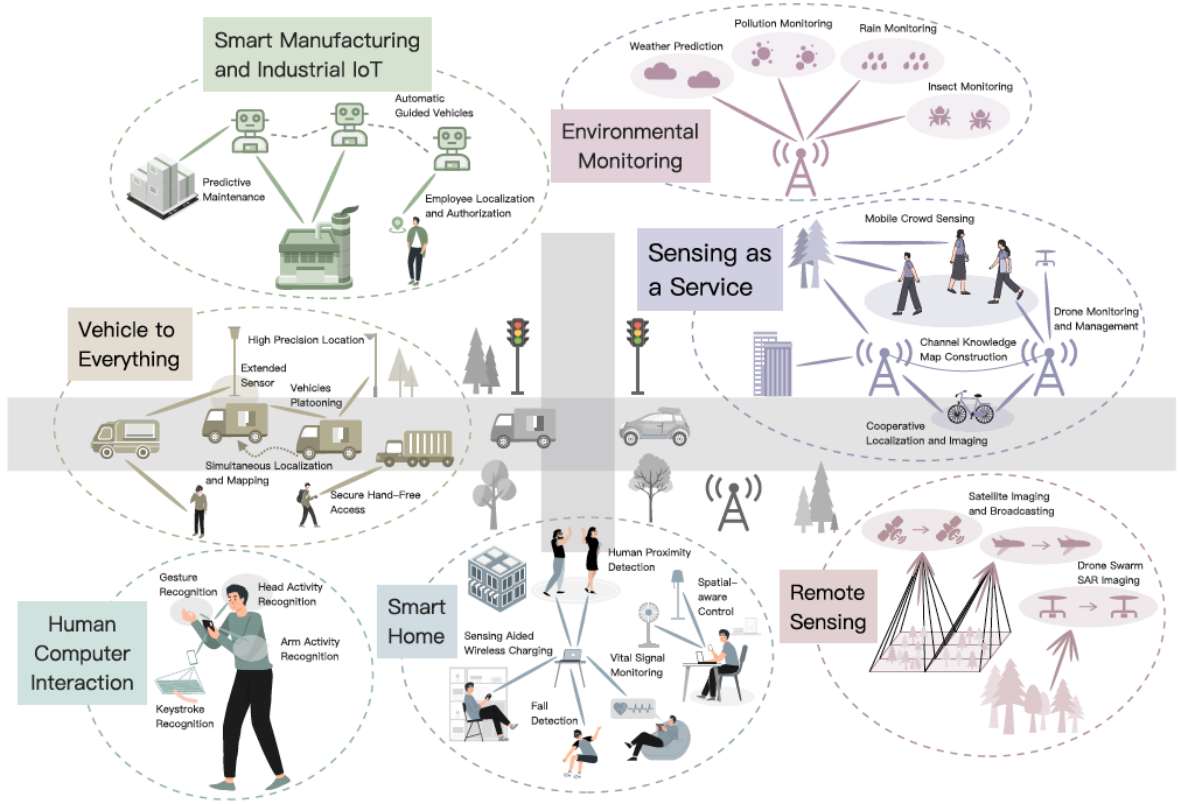

Fig. 1. ISAC technology for future wireless networks.

The ultimate goal is to ***co-design*** for mutual benefit

- Communication-assisted Sensing
- Sensing-assisted Communication

Fan Liu, Yuanhao Cui,Christos Masouros, Jie Xu,Tony Xiao Han, Yonina C. Eldar, Stefano Buzzi, "Integrated Sensing and Communications: Toward Dual-Functional Wireless Networks for 6G and Beyond," IEEE Journal on Selected Areas in Communications, vol. 40 (6) June 2022

IEEE VTS Connecting the Mobile World

Application Scenarios for UAV enabled Integrated Sensing and Communication

Track location of ground receivers for better beam tracking

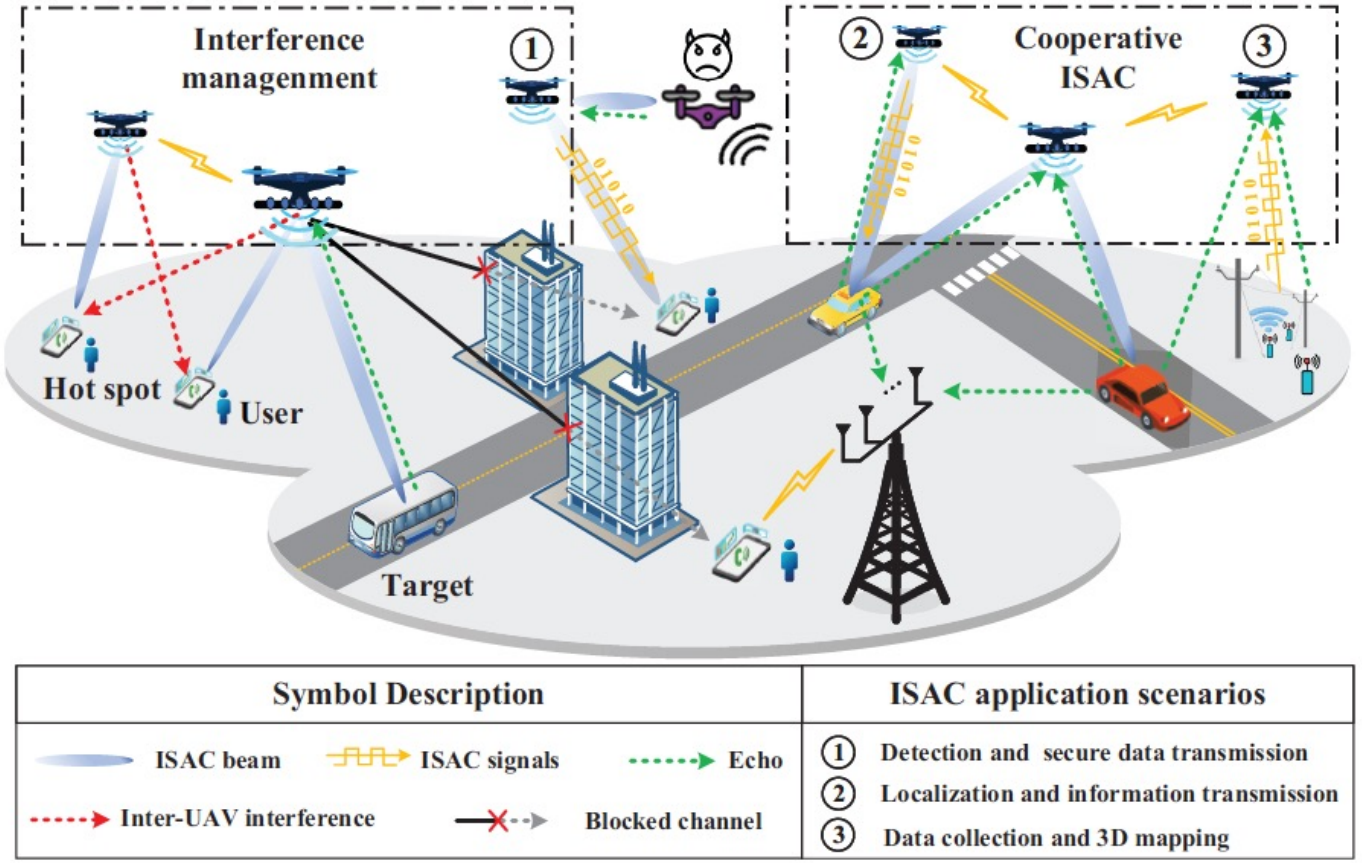

Fig. 1. Application scenarios for UAV-enabled ISAC.

Detect and monitor suspicious UAV targets

Aerial Relays to improve coverage

K. Meng *et al.*, "UAV-Enabled Integrated Sensing and Communication: Opportunities and Challenges," in *IEEE Wireless Communications*, April 2023 doi: 10.1109/MWC.131.2200442.

Drone Assisted Vehicular Networks

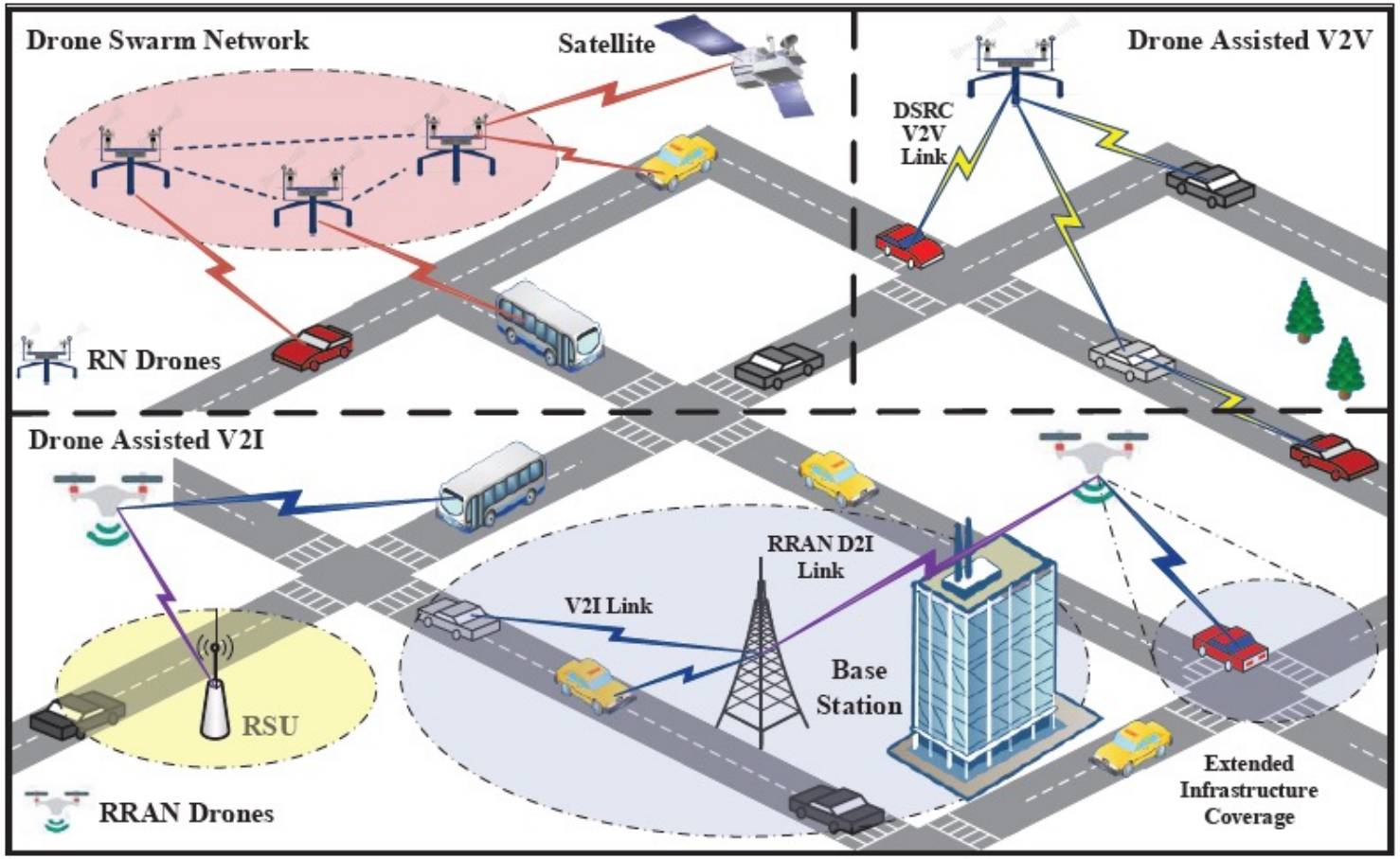

FIGURE 1. Drone Assisted Vehicular Networks architecture.

Line-of-Sight Links which can provide higher reliability and throughput

V2V and V2I connectivity can be enhanced significantly

W. Shi, H. Zhou, J. Li, W. Xu, N. Zhang and X. Shen, "Drone Assisted Vehicular Networks: Architecture, Challenges and Opportunities," in *IEEE Network*, vol. 32, no. 3, pp. 130-137, May/June 2018, doi: 10.1109/MNET.2017.1700206.

UAV Sensing and Transmission

1. UAV Sensing: In UAV sensing, the UAV first moves to the location that is suitable for sensing, and then hovers to perform data sensing for the task.

2. UAV Transmission: In UAV transmission, the UAV first moves to the area where the communication constraints are satisfied, and then transmits the sensory data to the BS.

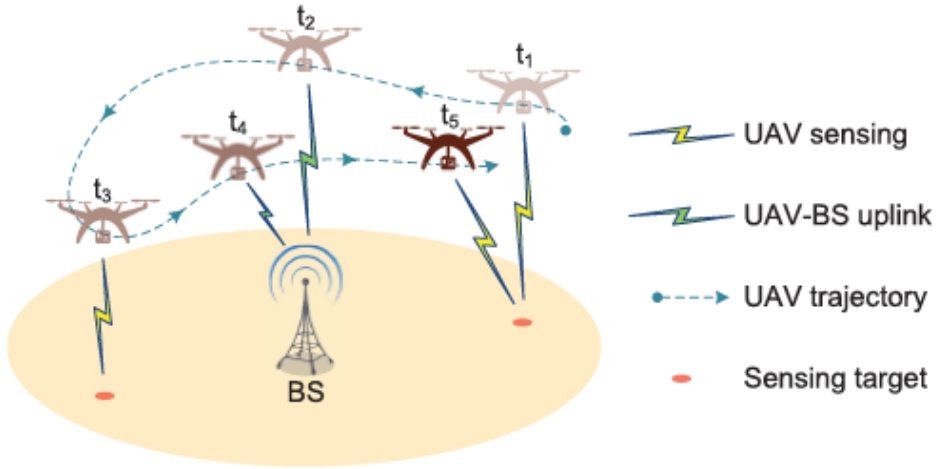

Fig. 1. System model of cellular Internet of UAVs.

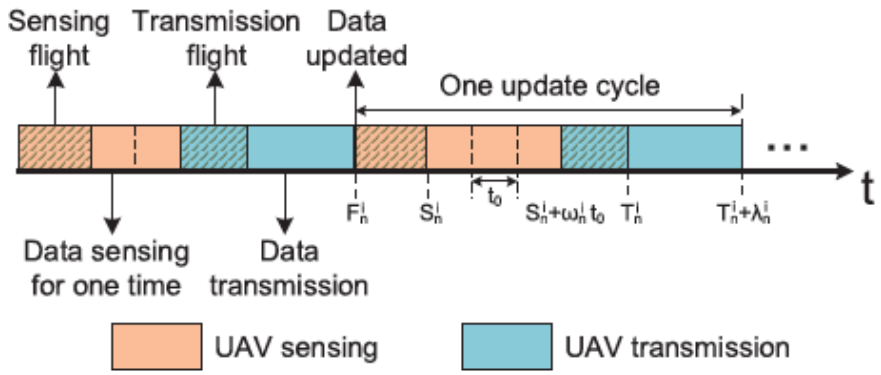

Fig. 2. UAV sensing and transmission procedures.

S. Zhang, H. Zhang, Z. Han, H. V. Poor and L. Song, "Age of Information in a Cellular Internet of UAVs: Sensing and Communication Trade-Off Design," in IEEE Transactions on Wireless Communications, vol. 19, no. 10, pp. 6578-6592, Oct. 2020, doi: 10.1109/TWC.2020.3004162.

Wireless Power Transfer and Path Planning for Precision Agriculture

- Charging Sensor Nodes (SNs) and collecting sensing data using UAVs. The problems of cluster head (CH) election and path planning are considered at the same time to maximize charging efficiency in a way that the lifetime of SNs can be prolonged.

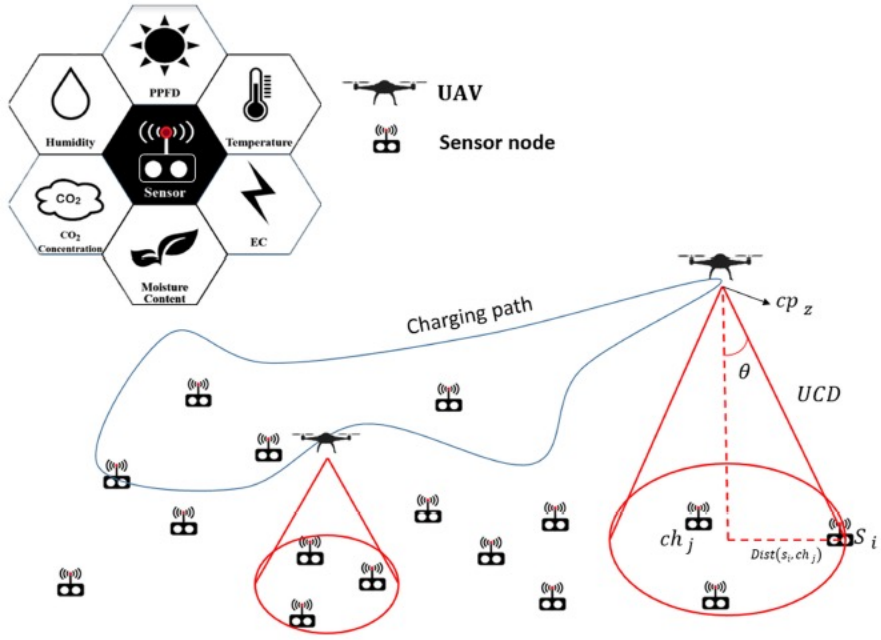

FIGURE 1. Network architecture.

W. -C. Chien, M. M. Hassan, A. Alsanad and G. Fortino, "UAV–Assisted Joint Wireless Power Transfer and Data Collection Mechanism for Sustainable Precision Agriculture in 5G," in IEEE Micro, vol. 42, no. 1, pp. 25-32, 1 Jan.-Feb. 2022, doi: 10.1109/MM.2021.3122553.

UAS related Remote Sensing

Synthetic Aperture Radar (SAR) systems carried by aerial platforms using chirp or OFDM waveforms.

Communication data can be embedded into these waveforms, to broadcast low-speed data streams

A radio sensing system and an emergency communication system can be merged to achieve higher energy and hardware efficiency

A swarm of drones can cooperatively act as mobile antenna array

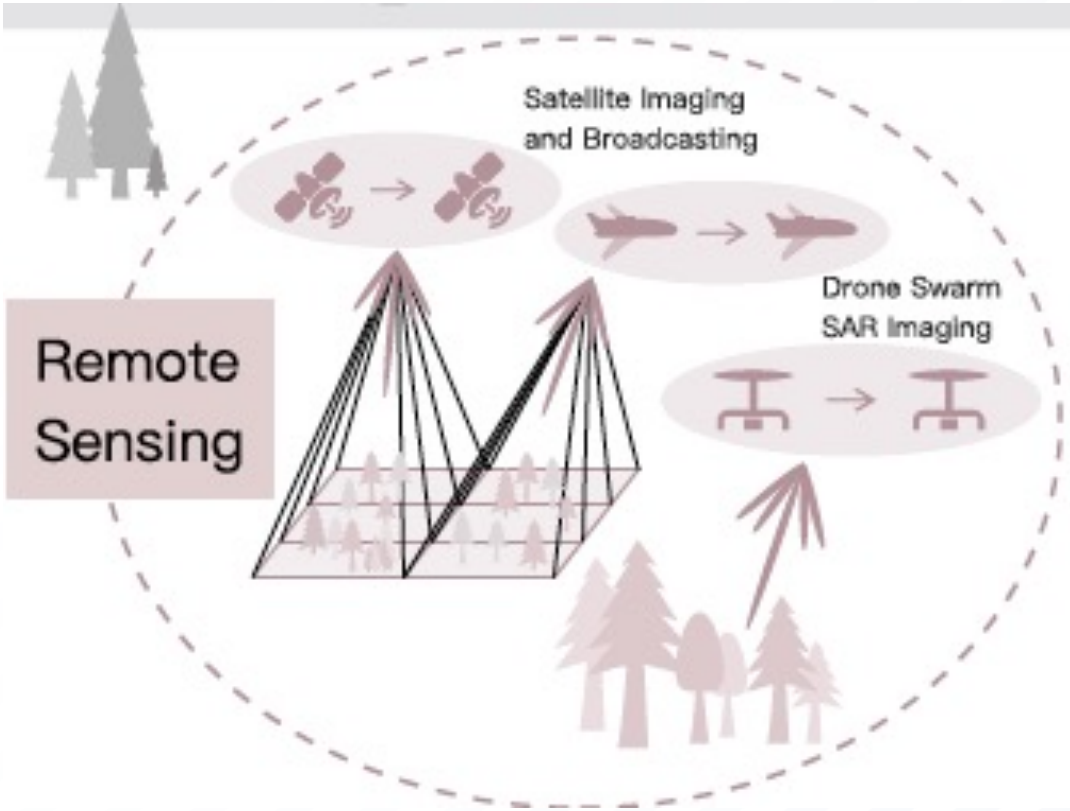

Fan Liu, Yuanhao Cui,Christos Masouros, Jie Xu,Tony Xiao Han, Yonina C. Eldar, Stefano Buzzi, "Integrated Sensing and Communications: Toward Dual-Functional Wireless Networks for 6G and Beyond," IEEE Journal on Selected Areas in Communications, vol. 40 (6) June 2022

Flying Radio Access Network (FRAN)

FRAN provides wireless connectivity to ground users by aerial base stations (BSs) that are mounted on unmanned aerial vehicles (UAVs) or balloons.

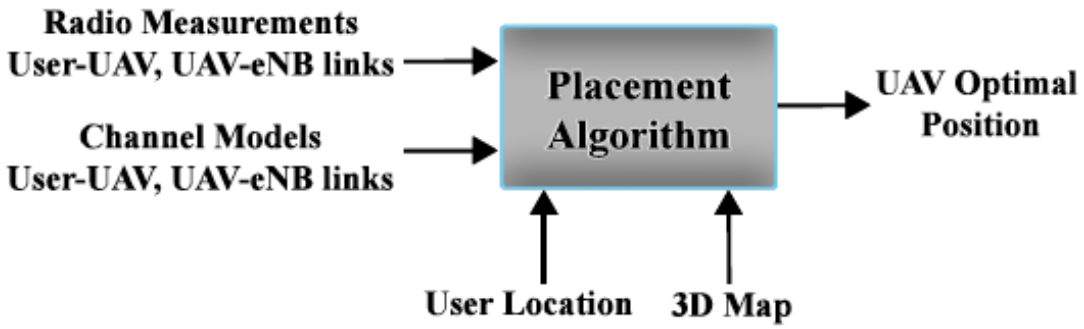

Figure 3: UAV placement algorithm.

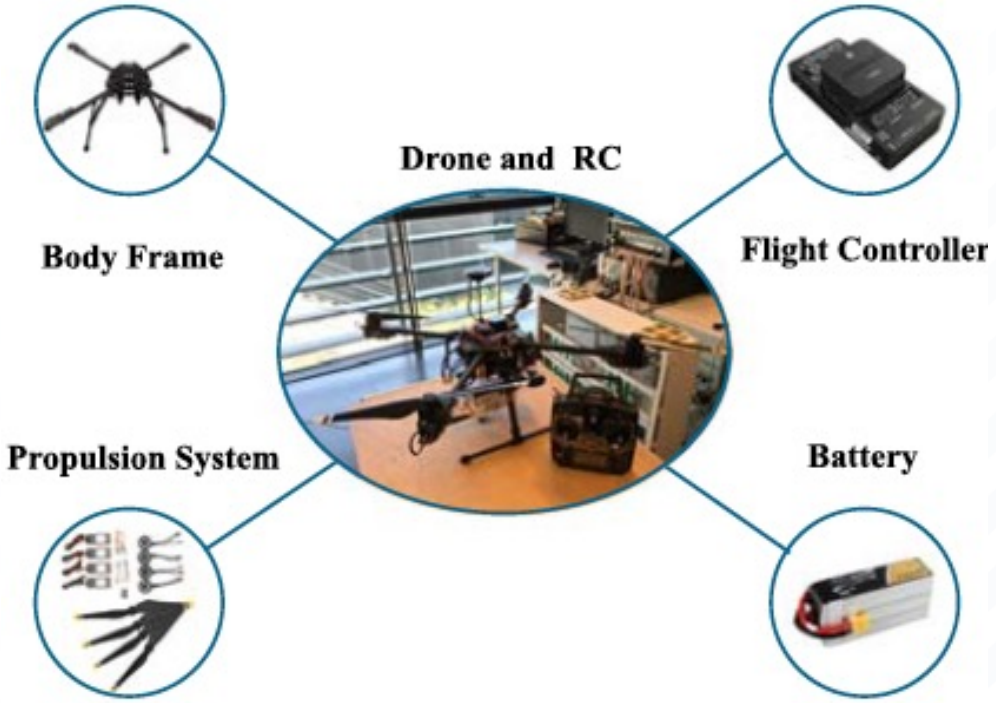

Figure 2: Custom-built UAV.

R. Gangula, O. Esrafilian, D. Gesbert, C. Roux, F. Kaltenberger and R. Knopp, "Flying Rebots: First Results on an Autonomous UAV-Based LTE Relay Using Open Airinterface," 2018 IEEE SPAWC, Kalamata, Greece, 2018, pp. 1-5, doi: 10.1109/SPAWC.2018.8445947.

REBOT: Relaying Robot

- Autonomous flight of an aerial 5G relay providing enhanced end-to-end 5G connectivity to ground users from a terrestrial base station with an autonomous placement algorithm.
  - custom-built drone and a 5G base station based on OpenAirInterface. The ground user carries a commercial 5G module (Quectel) terminal.

Video

R. Gangula, O. Esrafilian, D. Gesbert, C. Roux, F. Kaltenberger and R. Knopp, "Flying Rebots: First Results on an Autonomous UAV-Based LTE Relay Using Open Airinterface," 2018 IEEE SPAWC, Kalamata, Greece, 2018, pp. 1-5, doi: 10.1109/SPAWC.2018.8445947.

Radar and Communication Systems Inspire Each Other

- Triggered by MIMO communication techniques, co-located MIMO radar was proposed
- Joint Sensing and Communication schemes
  - Sensing-centric design: combining chirp signals with phase-shift keying (PSK) modulations
  - Communication-centric design: Using OFDM waveform for sensing
- *Convergence of the two technologies into systems and devices, that can serve sensing and communication with a single transmission*
  - Integration Gain attained by the shared use of wireless resources for dual purposes of S&C to alleviate duplication of transmissions, devices, and infrastructure
  - Coordination Gain attained from the mutual assistance between S&C

Characteristics of a Sensing System

- Sensing Performance Metrics: Detection, Estimation, and Recognition
  - Detection: Binary Hypothesis problem. Detection performance can be measured by **Probability of Detection, Probability of False Alarm.**
  - Estimation: Extracting distance/velocity/angle/quantity/size of the target(s). Estimation performance can be measured by the **Mean Squared Error (MSE) and Cramér-Rao Bound (CRB)**
  - Recognition: Defining what the target object is. Performance is based on **recognition accuracy**

Detection of UAS using mmWave Radar

Table 1: Radar Specifications

Parameters	
Operating Frequency Band	76-81GHz
Operating Waveform	FMCW
Transmitted Bandwidth	501MHz
Tx Power	12dBm
PRF	6KHz
Rx Noise Figure	15dB (77-81GHz)
Azimuth Coverage (3dB Beamwidth)	± 28deg
Elevation Coverage (3dB Beamwidth)	± 14deg
Probability of Detection (P_D)	0.9
Probability of False Alarm (P_{FA})	10e-6

Table 2: UAS Specifications

Parameters	
Diagonal Length	650mm
Max Range	2Km (LOS)
Max Speed	22m/s
Estimated RCS	-20dBsm
Hovering Time	16mins
Operating Frequency	5.725-5.825GHz

Radar board was on the Ground and the UAS was flying.

The maximum detection range observed in this test scenario was 40m.

Experiments at Airfield in Indian Institute of Science Bangalore.

13◦01’38.2’’N 77◦33’47.8’’E

.

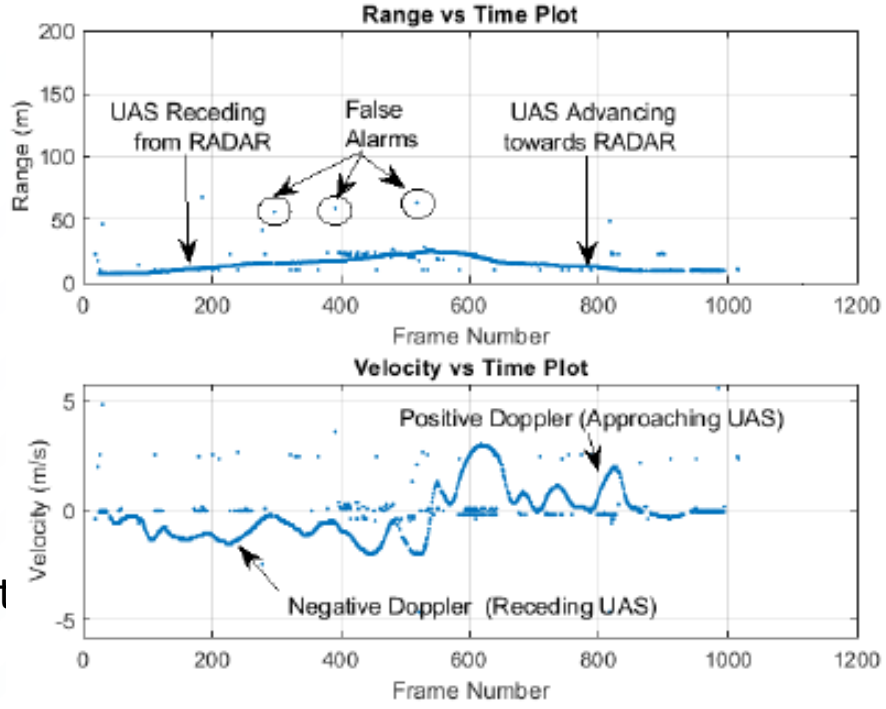

Fig. 3: Target Detections (Advancing and Receding UAS)

Peter Joseph Basil Morris and K.V.S Hari, “Detection and Localisation of Unmanned Aircraft Systems (UAS) using Millimeter Wave (mmWave) Automotive RADAR Sensors,” IEEE Sensors Letters, vol.5,No.6. June 2021.

IEEE VTS Connecting the Mobile World

Micro-Doppler Characteristics of UAS using mmWave Radar

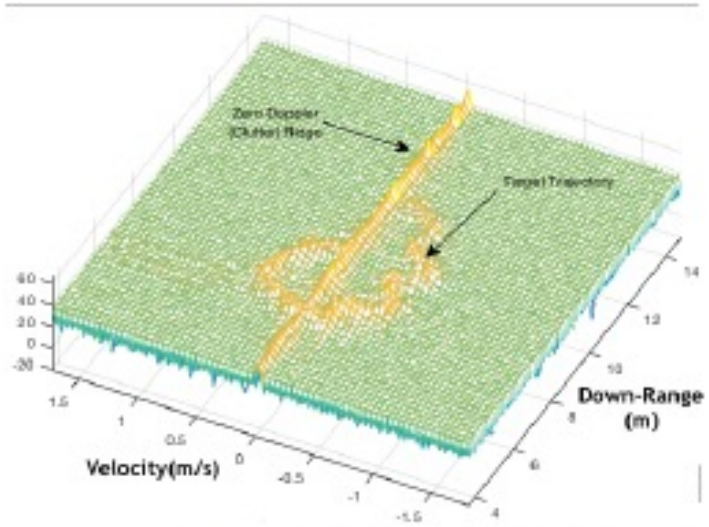

Fig. 4: Range-Doppler Map with UAS Trajectory

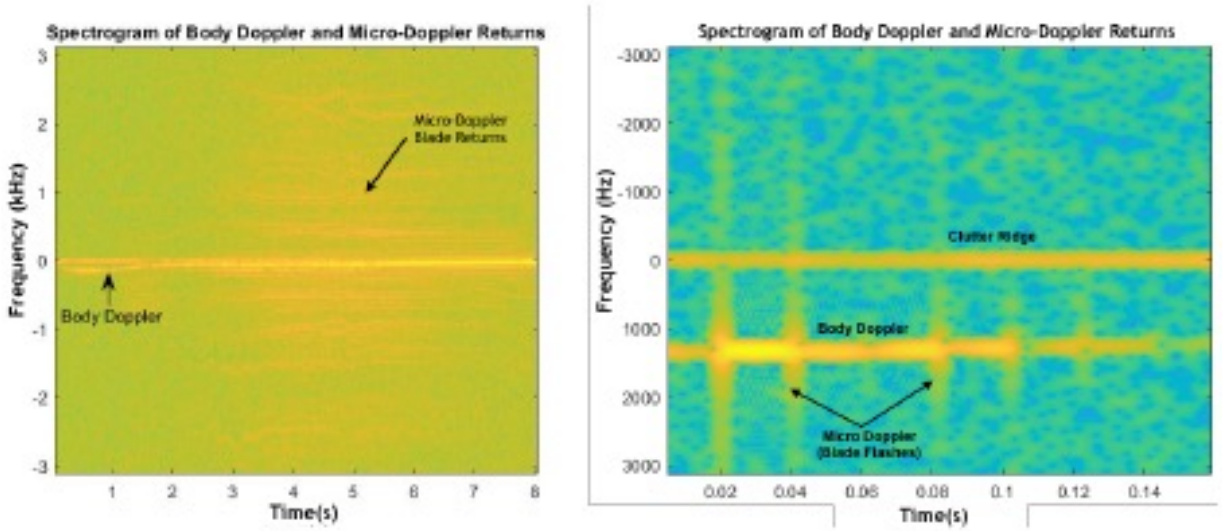

Fig. 8: Micro-Doppler Signatures From Spectrogram

Peter Joseph Basil Morris and K.V.S Hari, "Detection and Localisation of Unmanned Aircraft Systems (UAS) using Millimeter Wave (mmWave) Automotive RADAR Sensors," **IEEE Sensors Letters**, vol.5,No.6. June 2021.

Object Classification using Micro-Doppler Signature of UAS

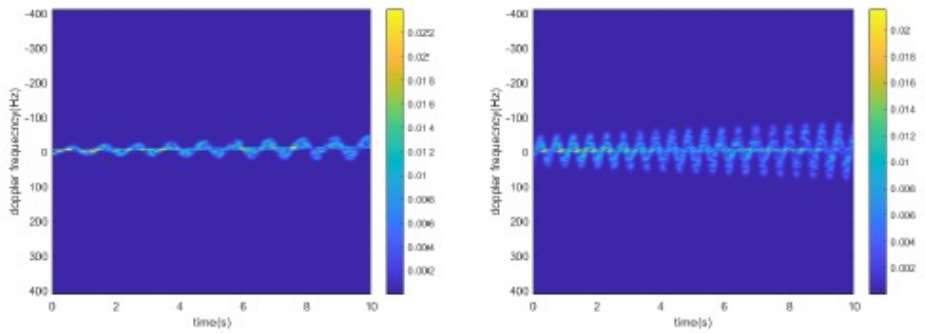

Fig. 3. Micro-Doppler with 1 Hz (left), 2 Hz (right) flapping frequency

TABLE II
ACCURACIES IN PERCENTAGE FOR 3 BIRDS,WITH FLAPPING FREQUENCIES 1 HZ, 2HZ, 1.5HZ

Classifier Name	Number of Pulses			
	4000	*6000*	*7000*	*10000*
SVM(Gaussian)	76.50	72.7	73.01	73.63
K-NN(K=5)	74.45	70.3	70.67	72.4

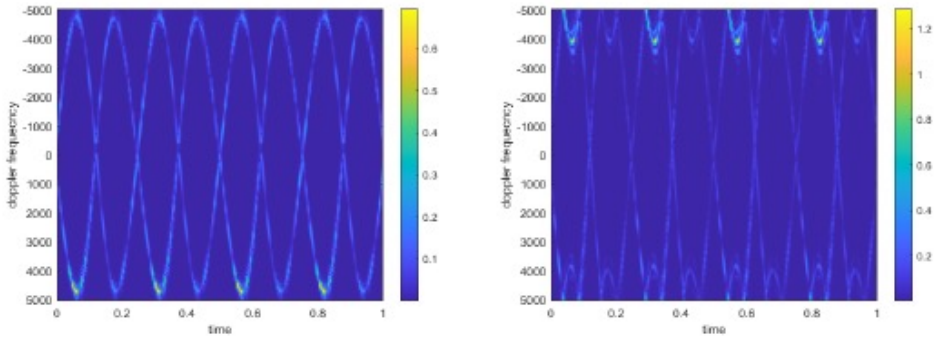

Fig. 5. Micro-Doppler Spectrogram of the UAV with Blade length 6m and 8 m

TABLE III
ACCURACIES IN PERCENTAGE FOR UAVS

Classifier Name	Number of Pulses		
	5000	*6000*	*8000*
SVM(rbf)	82	86.87	95.89
K-NN(K=5)	80.08	82.45	90.76

We consider two UAVs with rotors whose rotation rate is 4 rad/s and having blade lengths 6 m and 8m respectively. Both two-rotor systems are 1m wide. The operating frequency of the Radar is 5 GHz.

Titas Ghoshal, K.V.S. Hari, “Object Classification Using Micro-Doppler Signature And Clutter Suppression In MIMO Radar,” IEEE CONECCT, 2022.

IEEE VTS Connecting the Mobile World

Characteristics of Communication Sys

- Communication performance: Efficiency and Reliability
  - Efficiency: how much information is successfully delivered from the transmitter to the receiver, given limited available resources. **Spectral efficiency** (bit/s/Hz), **energy efficiency**, (bit/s/Joule), channel **capacity**, **coverage**, and the maximum number of **served users** are some metrics.
  - Reliability: ability of a communication system to reduce or even to correct erroneous information bits. Commonly used metrics include the **outage probability, bit error rate** (BER), symbol error rate (SER) and frame error rate (FER).

Information Theoretic Limits for Sensing & Communication Systems

$$\frac{d}{d\,\mathrm{snr}} I(\mathrm{snr}) = \frac{1}{2} MMSE(\mathrm{snr}). \quad (1)$$

That is, the derivative of the mutual information with respect to snr is equal to half of the MMSE regardless of the input statistics.

Dongning Guo, S. Shamai and S. Verdu, "Mutual information and minimum mean-square error in Gaussian channels," in *IEEE Transactions on Information Theory*, vol. 51, no. 4, pp. 1261-1282, April 2005, doi: 10.1109/TIT.2005.844072.

Tradeoff Between Capacity Metrics of Sensing and Communication

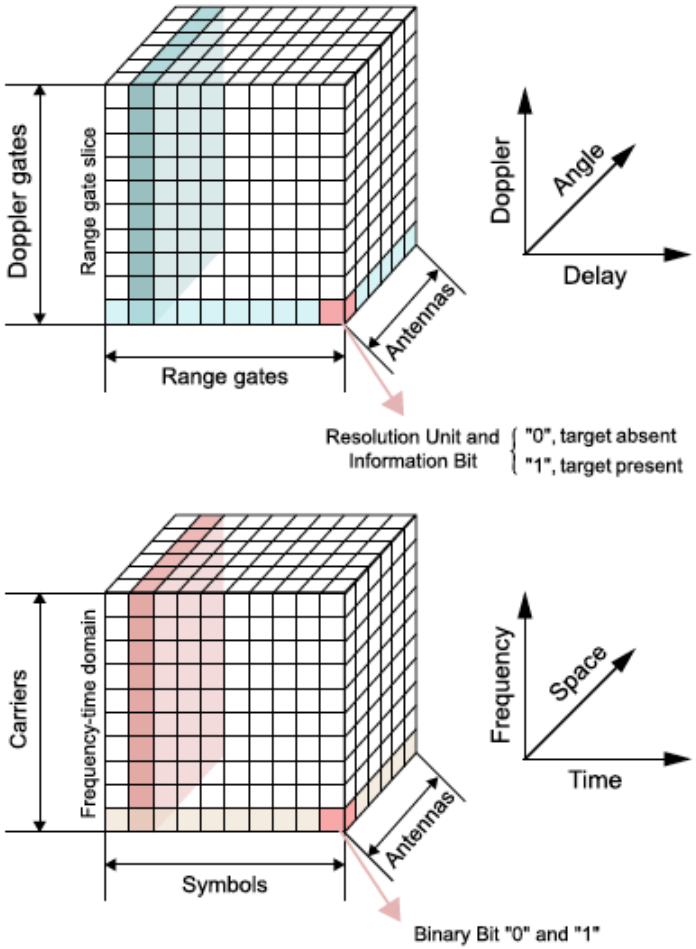

Fig. 6. Radar sensing resolution unit.

Each resolution unit can be considered as a binary information storage unit. Sensing capacity of an N_t antenna pulsed radar

$$C_R = \log N_u.$$

$$N_u \propto \left(\frac{D_{\max}}{\Delta D}\right)\left(\frac{2\pi}{\Delta\theta}\right)\left(\frac{PRF}{\Delta f_D}\right), \tag{20}$$

where ΔD, $\Delta\theta$, and Δf_D stand for the range resolution, angular resolution, and Doppler resolution of the radar, and $D_{\max}$ and PRF denote the maximum detectable range and the pulse repetition frequency (PRF), respectively.

$$\Delta D = \frac{c}{2B}, \quad \Delta f_D = \frac{1}{T_d}, \quad \Delta\theta \approx \frac{2}{N_t}, \tag{21}$$

where B is the bandwidth, and T_d represents the dwell time,

Fan Liu, Yuanhao Cui,Christos Masouros, Jie Xu,Tony Xiao Han, Yonina C. Eldar, Stefano Buzzi, "Integrated Sensing and Communications: Toward Dual-Functional Wireless Networks for 6G and Beyond," IEEE Journal on Selected Areas in Communications, vol. 40 (6) June 2022

MIMO-OFDM Radar and Communication Systems

J. A. Zhang et al., "An Overview of Signal Processing Techniques for Joint Communication and Radar Sensing," in IEEE Journal of Selected Topics in Signal Processing, vol. 15, no. 6, pp. 1295-1315, Nov. 2021, doi: 10.1109/JSTSP.2021.3113120.

OFDM - Recap

TIME SIGNAL

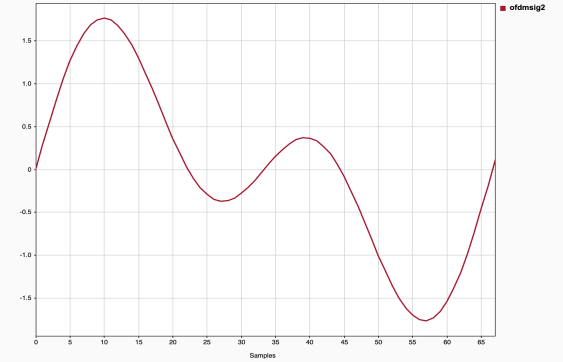

OFDM SYMBOL
with
2 Sub-Carriers

FREQUENCY SPECTRUM

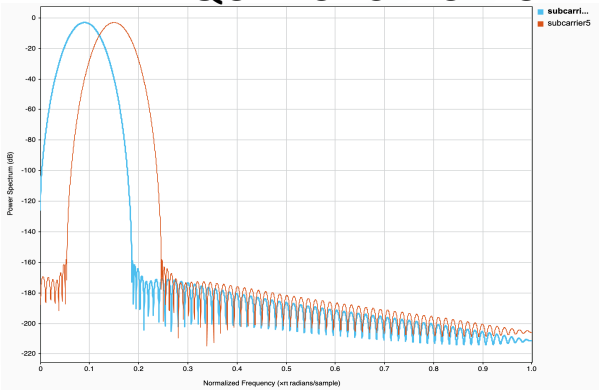

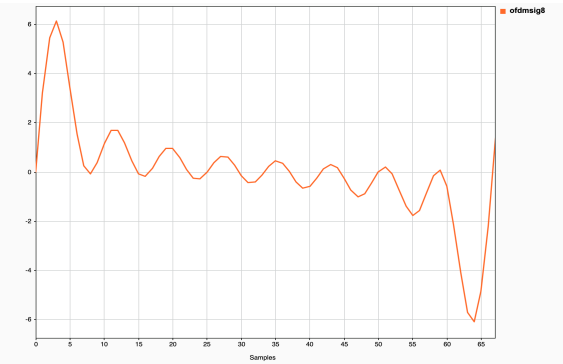

OFDM SYMBOL
with
8 Sub-Carriers

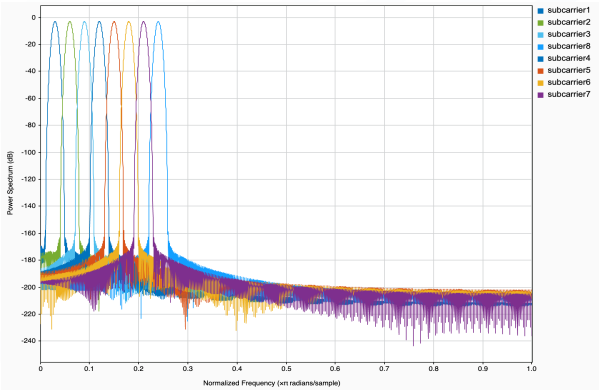

Peak-to-average Power Ratio (PAPR) is high

IEEE VTS Connecting the Mobile World

MIMO OFDM Communication System- Recap

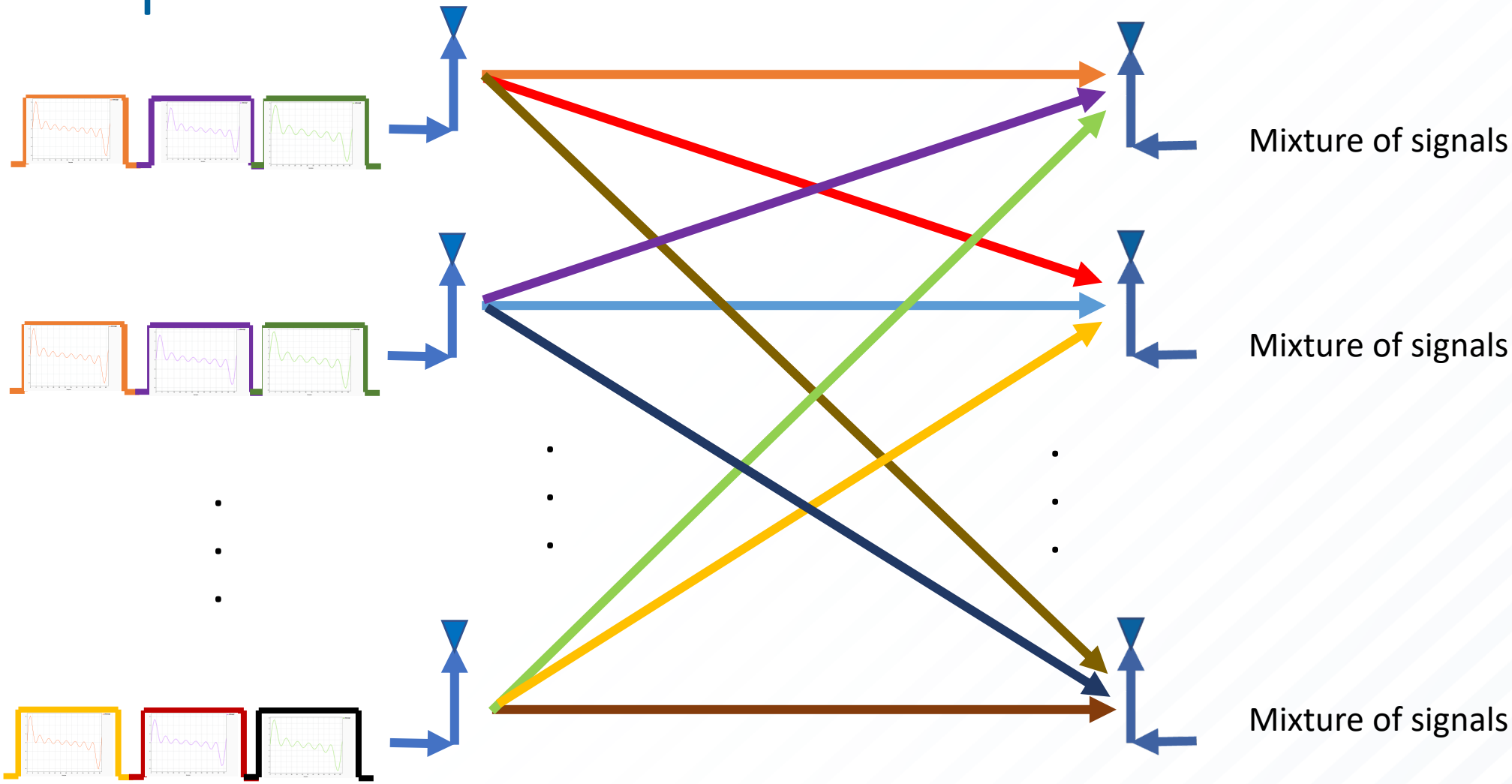

MIMO OFDM Communication System- Recap

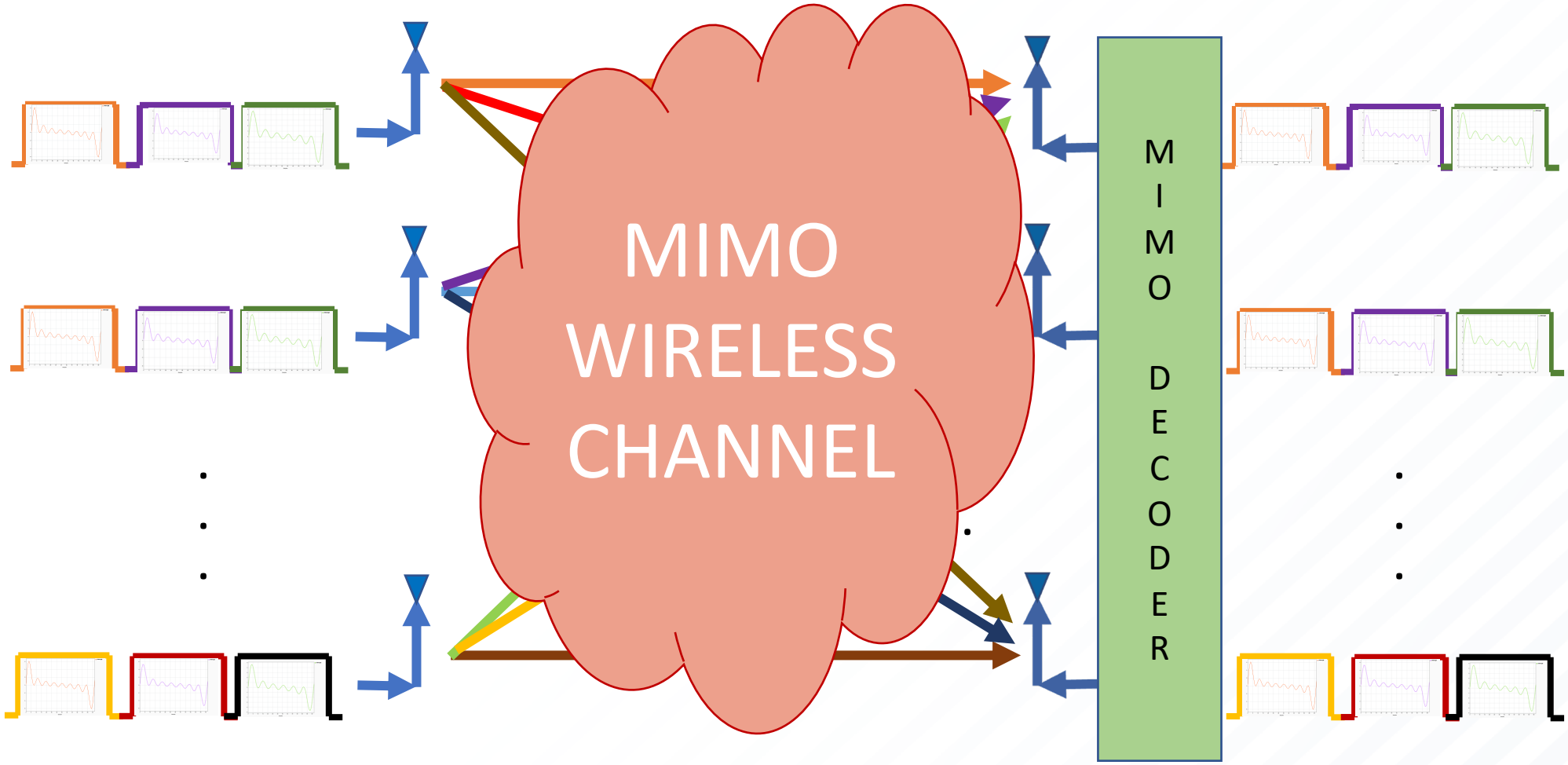

MIMO OFDM Radar System- Recap

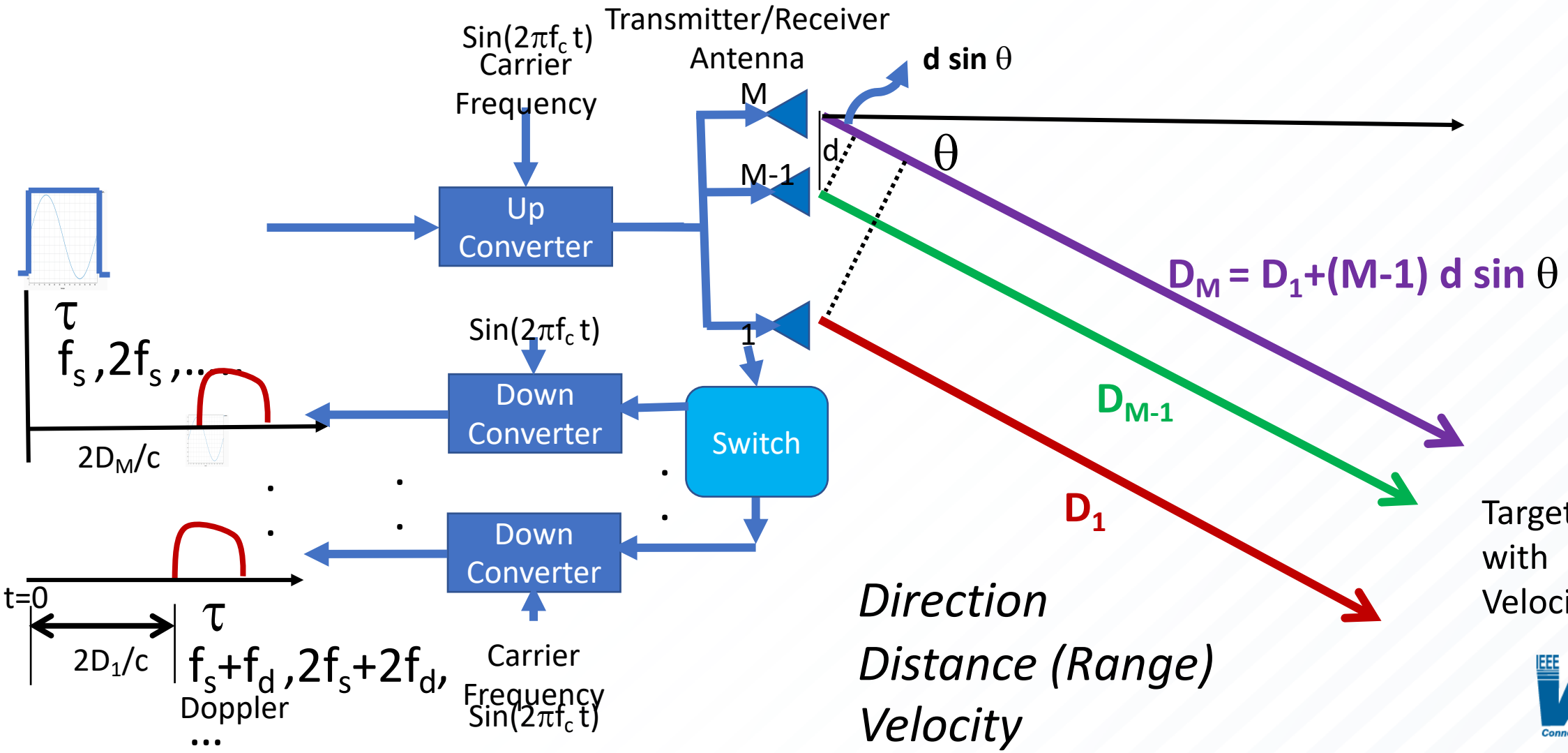

MIMO-OFDM Dual Function Radar Communication (DFRC) System

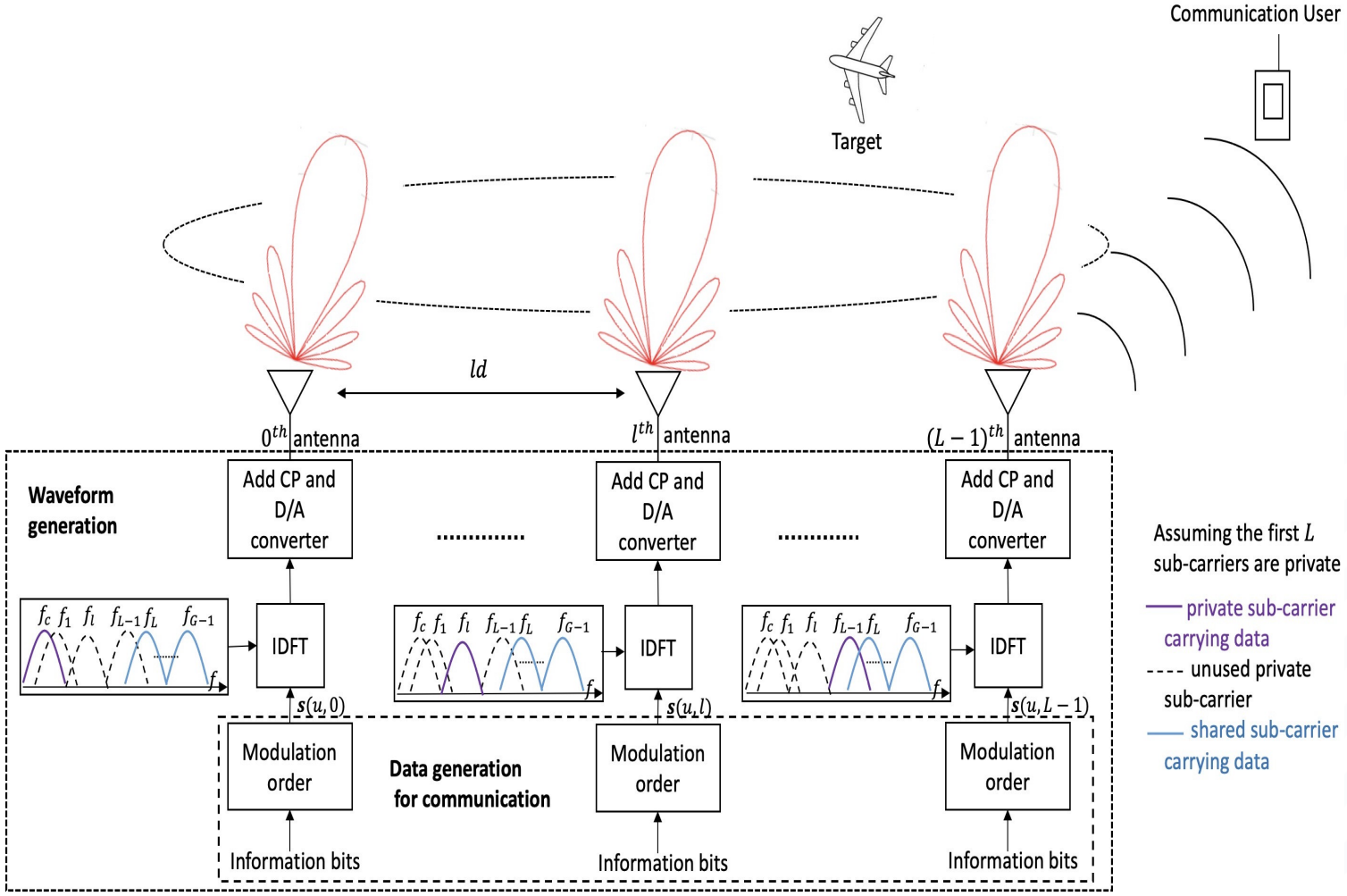

$\boldsymbol{s}(u,l)$ is a vector of transmitted symbols on all sub-carriers for u^{th} OFDM symbol and l^{th} transmit antenna

MIMO Shared Subcarriers-OFDM (SS-OFDM) System

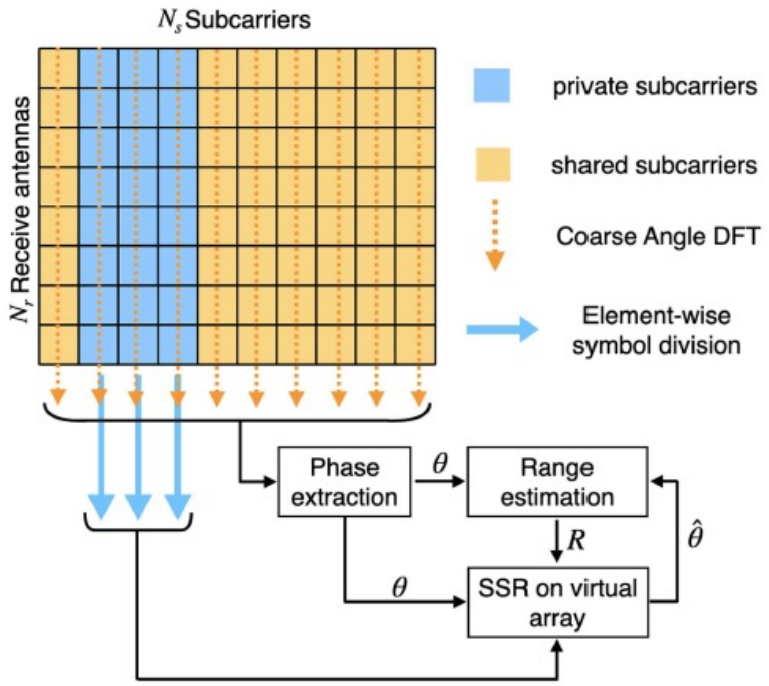

Fig. 2. Target estimation with private subcarriers in an SS-OFDM DFRC system.

- Transmits OFDM waveforms, where the subcarriers are marked as shared or private by allowing antennas to simultaneously transmit on all shared subcarriers. The private subcarriers are made available to the transmit antennas to transmit in an exclusive fashion.
- Flexibly trades off communication rate for improved target estimation performance by controlling the number of private subcarriers.

Z. Xu and A. Petropulu, "A Bandwidth Efficient Dual-Function Radar Communication System Based on a MIMO Radar Using OFDM Waveforms," in *IEEE Transactions on Signal Processing*, vol. 71, pp. 401-416, 2023, doi: 10.1109/TSP.2023.3241779.

Parameter Estimation in MIMO-OFDM DFRC System

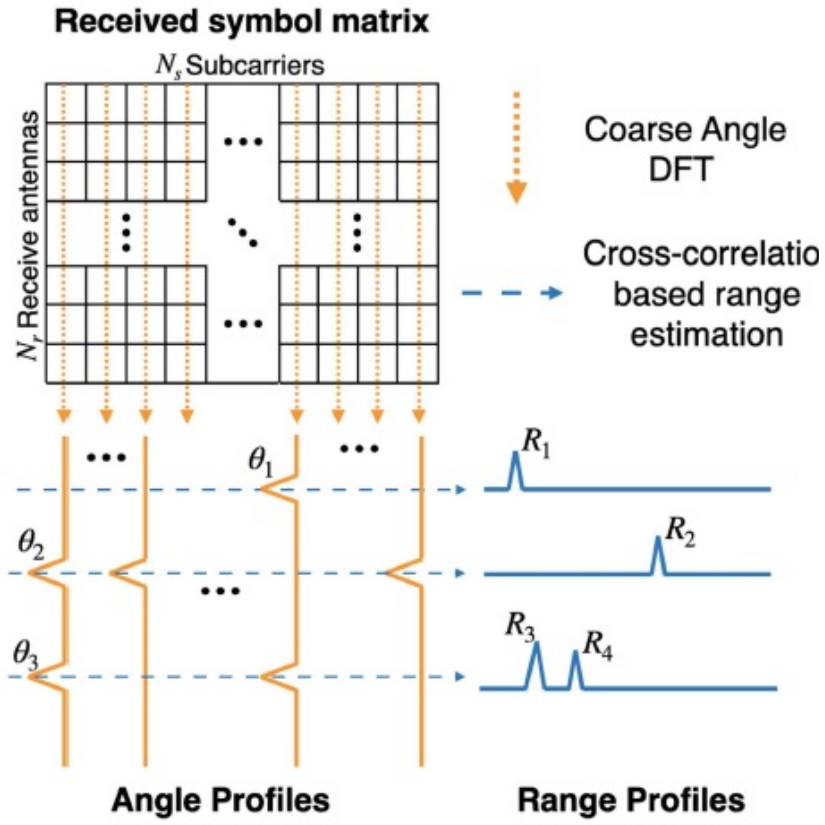

Fig. 1. Estimation of angle and range in one OFDM symbol.

DOA estimation:

$$y(g,u,m) = \sum_{k=1}^{K} \alpha_k A(k,g,u) e^{-jm\omega_k} \rightarrow \text{Fourier Analysis across the spatial domain} \rightarrow \{\widehat{\theta_k}\}_{k=1}^{K}$$

Similarly, Fourier Transform of sequences across the sub-carrier domain will provide Range estimates and Fourier transform across symbols will give velocity estimates

Z. Xu and A. Petropulu, "A Bandwidth Efficient Dual-Function Radar Communication System Based on a MIMO Radar Using OFDM Waveforms," in *IEEE Transactions on Signal Processing*, vol. 71, pp. 401-416, 2023, doi: 10.1109/TSP.2023.3241779.

Subspace Methods vs Fourier Transform Methods

- For a data model having a sum of exponentials
  - Fourier Transform methods do not perform well if the frequencies are very close
  - Subspace methods like ESPRIT, MUSIC, Root-MUSIC perform well
- Subspace methods require a certain structure in the data model

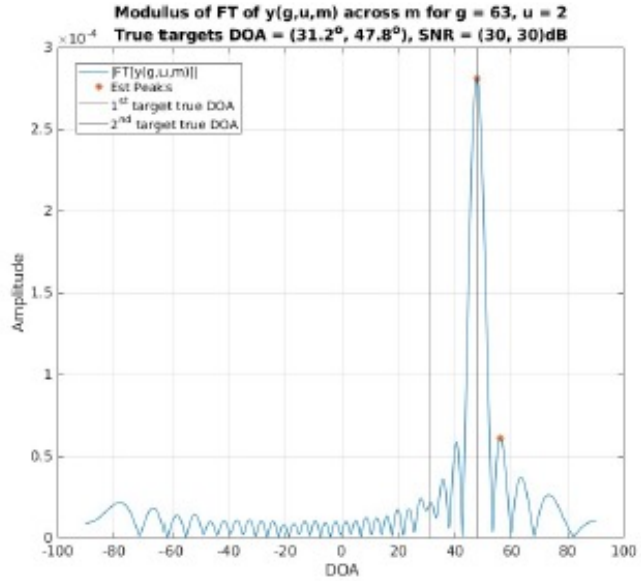

Fig. 2: Illustration where FT method is unable to identify the true peaks and consequently the DOAs of the targets

IEEE VTS Connecting the Mobile World

Proposed Subspace Approach to Estimate Range, Velocity and Direction

- Subspace Approach has been primarily used to estimate temporal frequencies or spatial frequencies (Directions of Arrival)
- Range and Velocity are estimated using the estimated Direction via the Fourier Transform approach
- **Novel waveform design** to enable subspace approach for estimating range and velocity also implying that estimation accuracy can be improved significantly!

Bhogavalli Satwika, K.V.S. Hari, Eric Grivel, Vincent Corretja, “Estimating the target parameters based on MIMO OFDM DFRC system using subspace methods,” EURASIP Signal Processing, March 2023

Data Model for a MIMO OFDM DFRC System

- For K targets, the received symbols in the frequency domain are given by [1]:

$$y(g,u,m) = \sum_{k=1}^{K} \alpha_k \left[\sum_{l=0}^{L-1} s(g,u,l) \exp\left(-j2\pi l d \sin\theta_k \frac{(f_c + g\Delta f)}{c} \right) \right] \quad (1)$$

$$\times \exp\left(-j2\pi m d \sin\theta_k \frac{(f_c + g\Delta f)}{c} \right) \exp\left(-j2\pi g \Delta f \frac{2D_k}{c} \right) \exp(j2\pi u T f_k^d)$$

θ_k- DOA of the k^{th} target; D_k- range of the k^{th} target; f_k^d- Doppler frequency of the k^{th} target

g is the gth subcarrier in the OFDM Symbol; u is the Uth OFDM Symbol; m is the mth antenna

g= 1,…G; u = 1,… U; m= 1,…M

[1] Bhogavalli Satwika, K.V.S. Hari, Eric Grivel, Vincent Corretja, “Estimating the target parameters based on MIMO OFDM DFRC system using subspace methods,” EURASIP Signal Processing, March 2023

Z. Xu and A. Petropulu, "A Bandwidth Efficient Dual-Function Radar Communication System Based on a MIMO Radar Using OFDM Waveforms," in *IEEE Transactions on Signal Processing*, vol. 71, pp. 401-416, 2023, doi: 10.1109/TSP.2023.3241779.

Insights for Range

- For K targets, the received symbols in the frequency domain are given by [1]:

$$y(g,u,m) = \sum_{k=1}^{K} \alpha_k \left[\sum_{l=0}^{L-1} s(g,u,l) \exp\left(-j2\pi l d \sin\theta_k \frac{(f_c + g\Delta f)}{c} \right) \right] \quad (1)$$

$$\times \exp\left(-j2\pi m d \sin\theta_k \frac{(f_c + g\Delta f)}{c} \right) \exp\left(-j2\pi g \Delta f \frac{2D_k}{c} \right) \exp(j2\pi u T f_k^d)$$

θ_k- DOA of the k^{th} target; D_k- range of the k^{th} target; f_k^d- Doppler frequency of the k^{th} target

The **target range** introduces a phase shift in the expression of the received signal, y(g, u,m) in the frequency domain, i.e., across g.

[1] Bhogavalli Satwika, K.V.S. Hari, Eric Grivel, Vincent Corretja, "Estimating the target parameters based on MIMO OFDM DFRC system using subspace methods," EURASIP Signal Processing, March 2023

Insights for Velocity

- For K targets, the received symbols in the frequency domain are given by [1]:

$$y(g,u,m) = \sum_{k=1}^{K} \alpha_k \left[\sum_{l=0}^{L-1} s(g,u,l) \exp\left(-j2\pi l d \sin\theta_k \frac{(f_c + g\Delta f)}{c} \right) \right] \quad (1)$$

$$\times \exp\left(-j2\pi m d \sin\theta_k \frac{(f_c + g\Delta f)}{c} \right) \exp\left(-j2\pi g \Delta f \frac{2D_k}{c} \right) \exp(j2\pi u T f_k^d)$$

θ_k- DOA of the k^{th} target; D_k- range of the k^{th} target; f_k^d- Doppler frequency of the k^{th} target

The **Doppler frequency or the velocity of the target** introduces a progressive phase shift in the expression of the received signal, y(g, u,m) along the time domain, i.e., along u.

[1] Bhogavalli Satwika, K.V.S. Hari, Eric Grivel, Vincent Corretja, "Estimating the target parameters based on MIMO OFDM DFRC system using subspace methods," EURASIP Signal Processing, March 2023

Insights from data model

- For K targets, the received symbols in the frequency domain are given by [1]:

$$y(g,u,m) = \sum_{k=1}^{K} \alpha_k \left[\sum_{l=0}^{L-1} s(g,u,l) \exp\left(-j2\pi l d \sin\theta_k \frac{(f_c + g\Delta f)}{c} \right) \right] \times \exp\left(-j2\pi m d \sin\theta_k \frac{(f_c + g\Delta f)}{c} \right) \exp\left(-j2\pi g \Delta f \frac{2D_k}{c} \right) \exp(j2\pi u T f_k^d) \quad (1)$$

θ_k- DOA of the k^{th} target; D_k- range of the k^{th} target; f_k^d- Doppler frequency of the k^{th} target

For a fixed sub-carrier and a fixed OFDM symbol, the **DOA of the target** introduces a progressive phase shift in the expression of the received signal, y(g, u,m) along the antennas in the spatial domain, i.e., along m.

[1] Bhogavalli Satwika, K.V.S. Hari, Eric Grivel, Vincent Corretja, "Estimating the target parameters based on MIMO OFDM DFRC system using subspace methods," EURASIP Signal Processing, March 2023

Novel Subspace Approach for Estimating Range

To estimate the range, the equation (7) can be rewritten as follows:

$$y(g,u,m) = \mathbf{a}_D^T(g)\boldsymbol{\Psi}(g,u,m)\mathbf{A}_\theta^T(g)\mathbf{s}(g,u) + \eta(g,u,m) \tag{20}$$

where $\mathbf{a}_D(g)$ is given by:

$$\mathbf{a}_D(g) = \left[\exp\left(-j2\pi g\Delta f\frac{2D_1}{c}\right) \quad \dots \quad \exp\left(-j2\pi g\Delta f\frac{2D_K}{c}\right)\right]^T \tag{21}$$

In addition, the matrix $\boldsymbol{\Psi}(g,u,m)$ is defined by:

$$\boldsymbol{\Psi}(g,u,m) = \tag{22}$$

$$\operatorname{diag}\left[\alpha_1\exp\left(j2\pi uTf_1^d\right)\exp(-jm\omega_1(g)) \ \dots \ \alpha_K\exp\left(j2\pi uTf_K^d\right)\exp(-jm\omega_K(g))\right]$$

[1] Bhogavalli Satwika, K.V.S. Hari, Eric Grivel, Vincent Corretja, "Estimating the target parameters based on MIMO OFDM DFRC system using subspace methods," EURASIP Signal Processing, March 2023

Proposed Waveform Design for Range

Assumption 1: Let us approximate f_g by f_c $\forall g = 0, 1, \cdots, G-1$. This approximation is valid as $\Delta f << f_c$ for any g. In that case, $\Psi(g, u, m)$ and $\mathbf{A}_\theta^T(g)$ no longer depend on g.

Assumption 2: For a fixed transmit antenna l, the data symbols transmitted on a fixed OFDM symbol u are assumed to be the same for all the sub-carriers for the subspace methods to be applicable. Mathematically, this means for $l = 0, 1, \cdots, L-1$ and $u = 0, 1, \cdots, U-1$:

$$s(0, u, l) = s(1, u, l) \cdots = s(G-1, u, l) \tag{23}$$

The vector $\mathbf{s}(g, u)$ is hence the same for all values of g and can be represented as $\mathbf{s}(u)$.

[1] Bhogavalli Satwika, K.V.S. Hari, Eric Grivel, Vincent Corretja, "Estimating the target parameters based on MIMO OFDM DFRC system using subspace methods," EURASIP Signal Processing, March 2023

Estimating Range

$$\mathbf{R}_D(u,m) \approx \sigma_s^2 \mathbf{A}_D(G)\boldsymbol{\Psi}(u,m)\mathbf{A}_\theta^T \mathbf{A}_\theta^* \boldsymbol{\Psi}^H(u,m)\mathbf{A}_D^H(G) + \sigma_\eta^2 \mathbf{I}_G$$

The matrices $\boldsymbol{\Psi}(u,m)$, $\mathbf{A}_D(G)$ and $\mathbf{A}_\theta$ have consequently a full rank, equal to K. The signal subspace associated with the correlation matrix equal to $\sigma_s^2 \mathbf{A}_D(G)\boldsymbol{\Psi}(u,m)\mathbf{A}_\theta^T \mathbf{A}_\theta^* \boldsymbol{\Psi}^H(u,m)\mathbf{A}_D^H(G)$ is of dimension K.

Therefore, the subspace methods like MUSIC , Root-MUSIC and ESPRIT are applicable to estimate the DOA of K targets from the full rank **correlation matrix $R_D(u,m)$.**

[1] Bhogavalli Satwika, K.V.S. Hari, Eric Grivel, Vincent Corretja, “Estimating the target parameters based on MIMO OFDM DFRC system using subspace methods,” EURASIP Signal Processing, March 2023

Novel Subspace Approach for Estimating Velocity

To estimate the target velocity, the equation (7) is written as:

$$y(g,u,m) = \mathbf{a}_v^T(u)\boldsymbol{\chi}(g,m)\mathbf{A}_\theta^T\mathbf{s}(g,u) + \eta(g,u,m) \tag{30}$$

where $\mathbf{a}_v(u)$ is given by:

$$\mathbf{a}_v(u) = \left[\exp\left(j2\pi uT f_1^d\right) \quad \dots \quad \exp\left(j2\pi uT f_K^d\right)\right]^T \tag{31}$$

Given ω_k whose expression is given in (11), the matrix $\boldsymbol{\chi}(g,m)$ is defined as:

$$\boldsymbol{\chi}(g,m) = \tag{32}$$

$$\operatorname{diag}\left[\alpha_1 \exp\left(-j2\pi g\Delta f\tfrac{2D_1}{c}\right)\exp\left(-jm\omega_1(g)\right) \quad \dots \quad \alpha_K \exp\left(-j2\pi g\Delta f\tfrac{2D_K}{c}\right)\exp\left(-jm\omega_K(g)\right)\right]$$

[1] Bhogavalli Satwika, K.V.S. Hari, Eric Grivel, Vincent Corretja, “Estimating the target parameters based on MIMO OFDM DFRC system using subspace methods,” EURASIP Signal Processing, March 2023

Waveform Design to Estimate Velocity

In the following, let us look at the assumption one could make to use subspace methods to estimate the velocity.

Assumption: For a fixed transmit antenna l, the data symbols transmitted on a fixed sub-carrier frequency f_g are assumed to be the same during all OFDM symbols for the subspace methods to be applicable. Mathematically, this means for $l = 0, 1, \cdots, L-1$ and $g = 0, 1, \cdots, G-1$:

$$s(g, 0, l) = s(g, 1, l) \cdots = s(g, U-1, l) \tag{33}$$

[1] Bhogavalli Satwika, K.V.S. Hari, Eric Grivel, Vincent Corretja, "Estimating the target parameters based on MIMO OFDM DFRC system using subspace methods," EURASIP Signal Processing, March 2023

Estimating Velocity

$$\mathbf{R}_v(g,m) = \sigma_s^2 \mathbf{A}_v(U)\boldsymbol{\chi}(g,m)\mathbf{A}_\theta^T \mathbf{A}_\theta^* \boldsymbol{\chi}^H(g,m)\mathbf{A}_v^H(U) + \sigma_\eta^2 \mathbf{I}_U$$

linearly independent. The matrices $\boldsymbol{\chi}(g,m)$, $\mathbf{A}_v(U)$ and $\mathbf{A}_\theta$ have consequently a full rank, equal to K. The signal subspace associated with the correlation matrix equal to $\sigma_s^2 \mathbf{A}_v(U)\boldsymbol{\chi}(g,m)\mathbf{A}_\theta^T \mathbf{A}_\theta^* \boldsymbol{\chi}^H(g,m)\mathbf{A}_v^H(U)$ is of dimension K. Therefore,

Therefore, the subspace methods like MUSIC , Root-MUSIC and ESPRIT are applicable to estimate the DOA of K targets from the full rank **correlation matrix $R_v(g,m)$.**

[1] Bhogavalli Satwika, K.V.S. Hari, Eric Grivel, Vincent Corretja, “Estimating the target parameters based on MIMO OFDM DFRC system using subspace methods,” EURASIP Signal Processing, March 2023

Estimating Direction

For example, the received data over the g^{th} sub-carrier related to the u^{th} OFDM symbol is stacked over the M antennas results in:

$$\mathbf{y}(g,u) = \begin{bmatrix} y(g,u,0) & \cdots & y(g,u,M-1) \end{bmatrix}^T \tag{8}$$

$$\mathbf{y}(g,u) = \mathbf{A}_\theta(g,M)\mathbf{\Phi}(g,u)\mathbf{A}_\theta^T(g,L)\mathbf{s}(g,u) + \boldsymbol{\eta}(g,u)$$

$$\begin{aligned} \mathbf{R}_\theta(g,u) &= \mathbb{E}[\mathbf{y}(g,u)\mathbf{y}^H(g,u)] \\ &= \mathbf{A}_\theta(g)\mathbf{\Phi}(g,u)\mathbf{A}_\theta^T(g)\mathbf{R}_s(g,u)\mathbf{A}_\theta^*(g)\mathbf{\Phi}^H(g,u)\mathbf{A}_\theta^H(g) + \sigma_\eta^2\mathbf{I}_M \end{aligned} \tag{17}$$

Therefore, the subspace methods like MUSIC , Root-MUSIC and ESPRIT are applicable to estimate the DOA of K targets from the full rank correlation matrix $R_\theta(g, u)$.

[1] Bhogavalli Satwika, K.V.S. Hari, Eric Grivel, Vincent Corretja, “Estimating the target parameters based on MIMO OFDM DFRC system using subspace methods,” EURASIP Signal Processing, March 2023

Parameters	Symbols	Parameters	Symbols
Number of transmit antennas	L	Velocity of the k^{th} target	v_k
Index of the transmit antenna	$l = 0, ..., L-1$	Doppler frequency of the k^{th} target	f_k^d
Number of receive antennas	M	Constellation order for modulation	B
Index of the receive antenna	$m = 0, ..., M-1$	Number of sub-carriers	G
Distance between two consecutive transmit/receive antennas	d	Index of the sub-carrier	$g = 0, ..., G-1$
Number of targets	K	Number of OFDM symbols	U
Index of the target	$k = 1, ..., K$	Index of the OFDM symbol	$u = 0, ..., U-1$
DOA of the k^{th} target	θ_k	Duration of the OFDM symbol	T
Range of the k^{th} target	D_k	Duration of the cyclic prefix	T_{CP}

Table 1: System parameters and the corresponding notations

[1] Bhogavalli Satwika, K.V.S. Hari, Eric Grivel, Vincent Corretja, “Estimating the target parameters based on MIMO OFDM DFRC system using subspace methods,” EURASIP Signal Processing, March 2023

Index	Assumption on transmitted data	Interpretation	Potential approaches that can be used to estimate DOA-range-velocity
Data Model 1	No assumption on $s(g,u,l) \forall g, u$ and l	The transmitted data are different over all sub-carriers, OFDM symbols and antennas. All sub-carriers are shared.	SS-TLS-TLS (proposed) FT-FT-FT [19]
Data Model 2	$s(0,u,l) = s(1,u,l) \cdots = s(G-1,u,l)$ $\forall u$ and l	The transmitted data are the same over all sub-carriers. All sub-carriers are shared.	SS-SS-TLS (proposed) SS-TLS-TLS (proposed) FT-FT-FT [19]
Data Model 3	$s(g,0,l) = s(g,1,l) \cdots = s(g,U-1,l)$ $\forall g$ and l	The transmitted data are the same over all OFDM symbols. All sub-carriers are shared.	SS-TLS-SS (proposed) SS-TLS-TLS (proposed) FT-FT-FT [19]
Data Model 4	$s(0,u,l) = s(1,u,l) \cdots = s(G-1,u,l)$ $= s(g,0,l) = s(g,1,l) \cdots = s(g,U-1,l)$ $\forall g, u,$ and l	The transmitted data are the same over all sub-carriers and all OFDM symbols. All sub-carriers are shared.	SS-SS-SS (proposed) SS-SS-TLS (proposed) SS-TLS-SS (proposed) SS-TLS-TLS (proposed) FT-FT-FT [19]
Data Model 5	Let $\mathbb{G}$ be the set of private sub-carriers. For $g \in \mathbb{G}$, $s(g,u,l) \neq 0$ if the g^{th} sub-carrier is paired to the l^{th} transmit antenna. Otherwise, $s(g,u,l) = 0$. For $g \notin \mathbb{G}$, no assumption on $s(g,u,l) \forall u \text{and} l$.	A set of L sub-carriers among G sub-carriers are private while remaining sub-carriers are shared. Data transmitted over all sub-carriers, OFDM symbols and transmit antennas are different.	Lasso-FT-FT [19] FT-FT-FT [19] SS-TLS-SS (proposed) SS-TLS-TLS (proposed)

Table 2: Assumptions on the transmitted data and corresponding usable approaches among the proposed and the existing approaches.

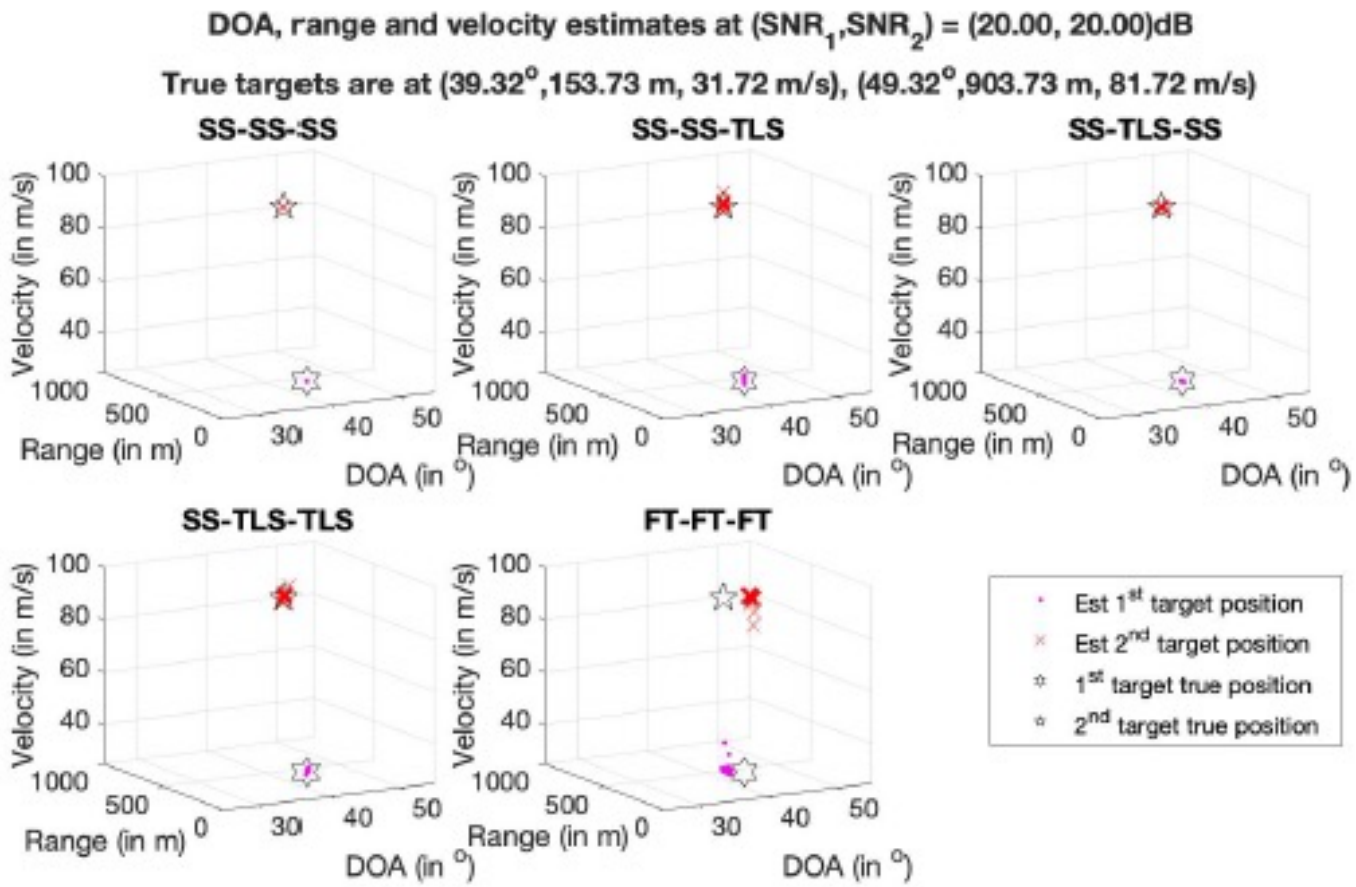

Figure 3: DOA, range and velocity estimates from SS-SS-SS, SS-SS-TLS, SS-TLS-SS, SS-TLS-TLS and FT-FT-FT based on data model 4 for 100 trials and 10 snapshots at $(\mathrm{SNR}_1, \mathrm{SNR}_2) = (20, 20)$ dB. True targets parameters are $(39.32^o, 153.73m, 31.72m/s)$ and $(49.32^o, 903.73m, 81.72m/s)$

[1] Bhogavalli Satwika, K.V.S. Hari, Eric Grivel, Vincent Corretja, "Estimating the target parameters based on MIMO OFDM DFRC system using subspace methods," EURASIP Signal Processing, March 2023

Summary

- Sharing the spectrum and hardware is critical for efficient use of resources
- Estimating the position and other relevant parameters of UAS is critical for joint sensing and communication networks

Open Problems to be addressed

- Correlation Model Between S&C Channels for sensing-assisted communication designs
- Quantitative Description of Coordination Gain
- ISAC Frame Protocol Design for unified ISAC waveforms or beams
- Joint Resource Allocation, Waveform, and Deployment/ Trajectory Design
- Coordinated Interference Management
- Cooperative ISAC
- IRS-assisted UAV-enabled ISAC
- Secure UAV ISAC
- AI for UAV ISAC Design
- …

THANK YOU

IEEE VTS Connecting the Mobile World

Join IEEE VTS at
www.vtsociety.org

Follow IEEE VTS on social media

Website
www.vtsociety.org

Facebook
facebook.com/IEEEVTS

Twitter
@IEEE_VTS

LinkedIn
www.linkedin.com/company/ieee-vehicular-technology-society